
^{18}F -FDG PET/CT, $^{99\text{m}}\text{Tc}$ -MIBI, and MRI in Evaluation of Patients with Multiple Myeloma

Rosa Fonti¹, Barbara Salvatore², Mario Quarantelli¹, Cesare Sirignano¹, Sabrina Segreto³, Fara PetruzzIELLO⁴, Lucio Catalano⁴, Raffaele Liuzzi¹, Bruno Rotoli⁴, Silvana Del Vecchio³, Leonardo Pace³, and Marco Salvatore³

¹Istituto di Biostrutture e Bioimmagini-CNR, Napoli, Italy; ²Fondazione SDN-IRCCS, Naples, Italy; ³Diagnostic Imaging Department, University Federico II, Naples, Italy; and ⁴Hematology Department, University Federico II, Naples, Italy

New imaging techniques have been introduced to assess the extent and severity of disease in multiple myeloma (MM) patients. The aim of our study was to compare newer imaging modalities—such as ^{18}F -FDG PET/CT, $^{99\text{m}}\text{Tc}$ -methoxyisobutylisonitrile ($^{99\text{m}}\text{Tc}$ -MIBI) scintigraphy, and MRI—to assess their relative contribution in the evaluation of MM patients at diagnosis. **Methods:** Thirty-three newly diagnosed patients with MM were prospectively studied. Diagnosis and staging were made according to standard criteria. All patients underwent whole-body ^{18}F -FDG PET/CT, whole-body $^{99\text{m}}\text{Tc}$ -MIBI, and MRI of the spine and pelvis within 10 d, and imaging findings were compared. **Results:** ^{18}F -FDG PET/CT was positive in 32 patients (16 focal uptake, 3 diffuse uptake, 13 focal and diffuse uptake), $^{99\text{m}}\text{Tc}$ -MIBI was positive in 30 patients (6 focal, 11 diffuse, 13 focal and diffuse uptake), and MRI of the spine and pelvis was positive in 27 patients (6 focal, 13 diffuse, 8 focal and diffuse uptake). ^{18}F -FDG PET/CT showed a total of 196 focal lesions (178 in bones and 18 in soft tissues), of which 121 were in districts other than the spine and pelvis, whereas $^{99\text{m}}\text{Tc}$ -MIBI visualized 63 focal lesions (60 in bones and 3 in soft tissues), of which 53 were in districts other than the spine and pelvis. In the spinal and pelvic regions, ^{18}F -FDG PET/CT detected 75 focal lesions (35 in spine and 40 in pelvis), $^{99\text{m}}\text{Tc}$ -MIBI visualized 10 focal lesions (1 in spine and 9 in pelvis), and MRI detected 51 focal lesions (40 in spine and 11 in pelvis). **Conclusion:** In whole-body analysis, ^{18}F -FDG PET/CT performed better than $^{99\text{m}}\text{Tc}$ -MIBI in the detection of focal lesions, whereas $^{99\text{m}}\text{Tc}$ -MIBI was superior in the visualization of diffuse disease. In the spine and pelvis, MRI was comparable to ^{18}F -FDG PET/CT and $^{99\text{m}}\text{Tc}$ -MIBI in the detection of focal and diffuse disease, respectively. Because myelomatous lesions may often occur out of spinal and pelvic regions, MRI should be reserved to the evaluation of bone marrow involvement of these districts, whereas ^{18}F -FDG PET/CT can significantly contribute to an accurate whole-body evaluation of MM patients. Finally, whole-body $^{99\text{m}}\text{Tc}$ -MIBI, despite its limited capacity in detecting focal lesions, may be an alternative option when a PET facility is not available.

Key Words: multiple myeloma; ^{18}F -FDG-PET/CT; $^{99\text{m}}\text{Tc}$ -MIBI; MRI

J Nucl Med 2008; 49:195–200

DOI: 10.2967/jnumed.107.045641

Multiple myeloma (MM) is a malignant hematologic disorder characterized by proliferation of clonal plasma cells and overproduction of monoclonal immunoglobulins (1). Diagnosis and staging of MM is based on standardized criteria, including plasma cell infiltration of bone marrow, osteolytic bone lesions, and a monoclonal component in serum or urine (2,3). At present, the most used system for staging MM is that introduced by Durie and Salmon several years ago (3). In this staging system myelomatous bone lesions are traditionally detected by a whole-body radiographic survey; however, radiographs can significantly underestimate the extent of bone and bone marrow involvement, especially in early phases of the disease (4). Therefore, more advanced imaging modalities—including whole-body ^{18}F -FDG PET/CT, whole-body $^{99\text{m}}\text{Tc}$ -methoxyisobutylisonitrile ($^{99\text{m}}\text{Tc}$ -MIBI) scintigraphy, and MRI—have been proposed in the effort to improve the management of MM patients in a noninvasive manner (5–7). ^{18}F -FDG PET/CT is a whole-body imaging technique capable of furnishing merged functional and morphologic information and is now routinely used in the staging and follow-up of lymphoma and various solid tumors. Moreover, previous studies have shown its usefulness in the detection of both osseous and extraosseous myeloma lesions (8–10). The lipophilic cation $^{99\text{m}}\text{Tc}$ -MIBI has been successfully used for the detection of a variety of neoplastic diseases, including multiple myeloma, where it is reported to be useful in the assessment of disease extension both at diagnosis and during follow-up (11–22). MRI allows a direct high-contrast and sensitive visualization of the bone marrow and its components and, therefore, has become the method of choice for bone marrow imaging (23,24). Recently, the Scientific Advisors of the International Myeloma Foundation proposed a new staging system called “Durie and Salmon PLUS” based on the traditional Durie and Salmon system integrated by ^{18}F -FDG PET or MRI of the

Received Jul. 26, 2007; revision accepted Oct. 29, 2007.

For correspondence or reprints contact: Rosa Fonti, MD, Istituto di Biostrutture e Bioimmagini-CNR, Via Pansini 5, 80131 Napoli, Italy.

E-mail: fontir@tin.it

COPYRIGHT © 2008 by the Society of Nuclear Medicine, Inc.

spine (25). This system attributes an equal relevance to both ^{18}F -FDG PET and MRI of the spine, which can be used, as suggested by the guidelines, in a flexible fashion. However, the relative contribution of each imaging technique, the specific clinical contexts in which one technique should be preferred over the other, or, eventually, the need to perform both imaging studies have not been fully elucidated. In addition, $^{99\text{m}}\text{Tc}$ -MIBI scans showed a high sensitivity and specificity in detecting sites of active disease and bone lesions (13). Despite several reports on the clinical usefulness of this imaging modality (11–22), it is still unclear whether $^{99\text{m}}\text{Tc}$ -MIBI can be fully replaced by ^{18}F -FDG PET/CT.

The aim of our study was to compare whole-body ^{18}F -FDG PET/CT with whole-body $^{99\text{m}}\text{Tc}$ -MIBI scintigraphy and MRI of the spine and pelvis to assess which of these imaging modalities would be more appropriate for detecting the presence of focal or diffuse disease and should, therefore, be included in the evaluation of patients with newly diagnosed MM.

MATERIALS AND METHODS

Thirty-three patients (11 females, 22 males; mean age \pm SD, 64 ± 12 y) with newly diagnosed MM according to standard criteria were enrolled in this prospective study, which had undergone institutional approval before its inception. After informed consent had been obtained, all patients underwent whole-body ^{18}F -FDG PET/CT, whole-body $^{99\text{m}}\text{Tc}$ -MIBI, and MRI of the spine and pelvis in a random order within a maximum interval of 10 d. None of the patients had undergone chemotherapy or radiotherapy before the study.

^{18}F -FDG PET/CT scans were acquired after fasting for 8 h and 60–90 min after intravenous administration of ^{18}F -FDG (350–370 MBq). The blood glucose level, measured just before tracer administration, was <120 mg/dL in all patients. ^{18}F -FDG PET/CT images were obtained using a PET/CT Discovery LS8 scanner (GE Healthcare). All scans were performed in 2-dimensional mode. An emission scan was performed in the caudocranial direction, from the upper thigh to the base of the skull (4 min/each bed position) and from the feet to the base of the thigh (2 min/each bed position). Iterative image reconstruction was completed with an ordered-subset expectation maximization (OSEM) algorithm (2 iterations, 28 subsets). CT with a 4-slice multidetector helical scanner was used (detector row configuration, 4×5 mm; pitch, 1.5; gantry rotation speed, 0.8 s per revolution; table speed, 30 mm per gantry rotation; 140 kV and 80 mA). Attenuation-corrected emission data were obtained using filtered backprojection CT reconstructed images (gaussian filter with 8-mm full width at half maximum) to match the PET resolution. Transaxial, sagittal, and coronal images and coregistered images were examined using Xeleris software (GE Healthcare). Focal areas visible on at least 2 contiguous PET slices—showing a maximum standardized uptake value (SUV_{max}) ≥ 2.5 and corresponding to CT abnormalities not attributable to benign bone pathologies—were considered to be sites of active disease. In particular, hypermetabolic sites corresponding to spondylopathy, osteoarthritis, joint disease, or traumas were carefully excluded from the analysis, whereas those corresponding to CT abnormalities—such as lytic lesions, minor lytic changes, osteopenic areas, morphologic changes not clearly attributable to degen-

erative disease, and minimal asymmetry of bone marrow attenuation likely due to plasma cell infiltration—were included.

$^{99\text{m}}\text{Tc}$ -MIBI imaging studies were performed by acquiring planar anterior and posterior whole-body scans (lasting about 10 min) 10 min after intravenous injection of 555 MBq of $^{99\text{m}}\text{Tc}$ -MIBI using a dual-head γ -camera (ECAM; Siemens), equipped with a low-energy, high-resolution collimator.

MRI studies were performed at 1.5 T (Achieva; Philips) along sagittal planes covering the whole spine with 3 partially overlapping slabs and along coronal planes for the study of the pelvis. MRI sequences included T1- and T2-weighted turbo-spin-echo images (with and without fat suppression by a preparatory pulse with spectral inversion [SPIR]) and postcontrast T1-weighted fat-suppressed turbo-spin-echo images (5 min after intravenous administration of 0.1 mmol/g gadopentetate dimeglumine [Magnevist]; Schering). The sequence parameters (repetition time/echo time/echo train length) used for the spine were 477/13/4 for T1-weighted images and 3,500/120/43 for T2-weighted images. The sequence parameters used for the pelvis were 550/14/5 for T1-weighted images and 3,500/120/43 for T2-weighted images with SPIR fat suppression. The whole study lasted approximately 35 min, including patient positioning.

^{18}F -FDG PET/CT, $^{99\text{m}}\text{Tc}$ -MIBI, and MRI were read and interpreted by 2 independent nuclear medicine physicians or 2 independent radiologists who were unaware of the imaging results. The data obtained were compared by using a χ^2 test or a Fisher exact test as appropriate. A probability value ≤ 0.05 was considered statistically significant. When a focal pattern was detected, the number and site of focal bone or soft-tissue lesions were reported. The number of focal lesions detected in each patient by each one of the 3 imaging techniques was compared by using the nonparametric paired-data Kendall's coefficient-of-concordance (*W*) test. A probability value ≤ 0.01 was considered statistically significant.

RESULTS

The results of whole-body ^{18}F -FDG PET/CT, whole-body $^{99\text{m}}\text{Tc}$ -MIBI, and MRI of the spine and pelvis performed on the 33 MM patients were compared according to the presence of a normal, diffuse, or focal (combination with or without diffuse) pattern of bone marrow involvement as shown in Table 1. Whole-body ^{18}F -FDG PET/CT was positive in 32 patients (97%), 3 (9%) of whom had a pure diffuse pattern of

TABLE 1

Whole-Body ^{18}F -FDG PET/CT, Whole-Body $^{99\text{m}}\text{Tc}$ -MIBI, and MRI of Spine and Pelvis Performed on 33 MM Patients at Diagnosis: Comparison According to Presence of Normal, Diffuse, or Focal and Focal + Diffuse Pattern of Bone Marrow Involvement

Imaging modality	N	D	F-FD
Whole-body ^{18}F -FDG PET/CT	1 (3)	3 (9)	29 (88)
Whole-body $^{99\text{m}}\text{Tc}$ -MIBI	3 (9)	11 (33)	19 (57)
MRI of spine and pelvis	6 (18)	13 (39)	14 (42)

N = normal; D = diffuse; F-FD = focal and focal + diffuse. Values in parentheses are percentages (2-sided Fisher exact test; $P < 0.005$).

bone marrow uptake, whereas 29 (88%) showed focal lesions in the presence (13 patients, 39%) or absence (16 patients, 48%) of diffuse uptake. Whole-body ^{99m}Tc -MIBI was positive in 30 patients (91%), of whom 11 (33%) presented a diffuse pattern of uptake and 19 (57%) showed a focal pattern with (13 patients, 39%) or without (6 patients, 18%) the association of diffuse uptake. MRI of the spine and pelvis was positive in 27 patients (81%), of whom 13 (39%) had a diffuse pattern and 14 (42%) showed a focal pattern, in combination with a diffuse pattern (8 patients, 24%) or alone (6 patients, 18%).

Comparing the pattern of bone marrow involvement obtained by ^{18}F -FDG PET/CT, ^{99m}Tc -MIBI, and MRI, using the Fisher exact test, a significant statistical difference ($P < 0.005$) between the 3 imaging methods was found. In particular, ^{18}F -FDG PET/CT detected a focal pattern, alone or combined with a diffuse pattern, with a higher frequency than ^{99m}Tc -MIBI ($P < 0.05$) and MRI ($P < 0.001$). On the other hand, ^{99m}Tc -MIBI and MRI were comparable and performed better than ^{18}F -FDG PET/CT in the detection of a pure diffuse pattern. By analyzing the number and sites of focal lesions detected, we found that ^{18}F -FDG PET/CT showed a total of 196 focal lesions, of which 75 were in the spine and pelvis (35 and 40, respectively) and 121 were in other districts, whereas ^{99m}Tc -MIBI visualized a total of 63 focal lesions, of which only 1 was in the spine, 9 were in the pelvis, and 53 were in other districts. Eighteen of the total focal lesions visualized by ^{18}F -FDG PET/CT and only 3 of the lesions detected by ^{99m}Tc -MIBI were localized in soft tissues. Finally, MRI detected a total of 51 focal lesions—40 in the spine and 11 in the pelvis. Comparing the number of focal lesions per patient detected by each imaging method on the whole dataset, using the nonparametric paired-data Kendall's W test, we showed that ^{18}F -FDG PET/CT visualized more focal lesions (5.94 ± 9.29) than ^{99m}Tc -MIBI and MRI (1.91 ± 4.45 and 1.54 ± 2.45 , respectively), with a significant statistical difference ($P < 0.001$) as shown in Table 2. We also performed a post hoc analysis using the Kendall's W test with Bonferroni correction and found a significant statistical difference between the number of focal lesions per patient detected by ^{18}F -FDG PET/CT and both ^{99m}Tc -MIBI ($P < 0.001$) and MRI ($P < 0.005$).

TABLE 2

Comparison of Number of Focal Lesions per Patient Detected by Whole-Body ^{18}F -FDG PET/CT, Whole-Body ^{99m}Tc -MIBI, and MRI of Spine and Pelvis

Focal lesions per patient (n)				Kendall's W test
Whole-body ^{18}F -FDG PET/CT	Whole-body ^{99m}Tc -MIBI	MRI spine and pelvis		
$5.94 \pm 9.29^{*†}$	1.91 ± 4.45	1.54 ± 2.45		$P < 0.001$

* $P < 0.001$, ^{18}F -FDG PET/CT vs. ^{99m}Tc -MIBI.

† $P < 0.005$, ^{18}F -FDG PET/CT vs. MRI.

TABLE 3

^{18}F -FDG PET/CT, ^{99m}Tc -MIBI, and MRI of Spinal and Pelvic District Performed on 33 MM Patients at Diagnosis: Comparison According to Presence of Normal, Diffuse, or Focal and Focal + Diffuse Pattern of Bone Marrow Involvement

Imaging modality	N	D	F-FD
Whole-body ^{18}F -FDG PET/CT of spine and pelvis	12 (36)	6 (18)	15 (45)
Whole-body ^{99m}Tc -MIBI of spine and pelvis	8 (24)	18 (54)	7 (21)
MRI of spine and pelvis	6 (18)	13 (39)	14 (42)

N = normal; D = diffuse; F-FD = focal and focal + diffuse. Values in parentheses are percentages (2-sided Fisher exact test; $P < 0.005$).

To compare homogeneously the 3 imaging methods used, we focused our analysis exclusively on the data obtained in the spinal and pelvic district as shown in Table 3. Comparing these data, using the Fisher exact test, we also found a significant statistical difference ($P < 0.05$) between the 3 imaging techniques. In particular, ^{18}F -FDG PET/CT and MRI were comparable and performed better than ^{99m}Tc -MIBI in the detection of a focal pattern, alone or combined with a diffuse pattern. On the other hand, ^{99m}Tc -MIBI and MRI were comparable and performed better than ^{18}F -FDG PET/CT in the detection of a diffuse pattern. However, these differences were statistically significant only between ^{18}F -FDG PET/CT and ^{99m}Tc -MIBI ($P < 0.01$). Comparing the number of focal lesions per patient visualized by each imaging technique exclusively in the spinal and pelvic district, using the nonparametric paired-data Kendall's W test, we found that ^{18}F -FDG PET/CT and MRI showed more focal lesions (2.27 ± 4.64 and 1.54 ± 2.45 , respectively) compared with ^{99m}Tc -MIBI (0.30 ± 0.68), with a significant statistical difference ($P < 0.005$) as shown in Table 4. Moreover, the post hoc analysis performed by using the Kendall's W test with Bonferroni correction showed a significant statistical difference between the number of focal lesions per patient detected by ^{18}F -FDG PET/CT and MRI ($P < 0.001$ and

TABLE 4

Comparison of Number of Focal Lesions per Patient Detected by ^{18}F -FDG PET/CT, ^{99m}Tc -MIBI, and MRI of Spinal and Pelvic District

Focal lesions per patient (n)				Kendall's W test
^{18}F -FDG PET/CT spine and pelvis	^{99m}Tc -MIBI spine and pelvis	MRI spine and pelvis		
$2.27 \pm 4.64^*$	0.30 ± 0.68	$1.54 \pm 2.45^†$		$P < 0.005$

* $P < 0.001$, ^{18}F -FDG PET/CT vs. ^{99m}Tc -MIBI.

† $P < 0.01$, MRI vs. ^{99m}Tc -MIBI.

$P < 0.01$, respectively) versus ^{99m}Tc -MIBI, whereas no significant statistical difference was found between ^{18}F -FDG PET/CT and MRI.

Finally, ^{18}F -FDG PET/CT, ^{99m}Tc -MIBI, and MRI influenced the subsequent clinical management in 18% of patients. In particular, ^{18}F -FDG PET/CT alone or in combination with ^{99m}Tc -MIBI upstaged and, consequently, modified the clinical management in 4 patients, whereas ^{99m}Tc -MIBI alone and MRI alone modified the clinical management in 1 patient each.

DISCUSSION

The results of the present study indicate that ^{18}F -FDG PET/CT performs better than both ^{99m}Tc -MIBI and MRI in the detection of focal lesions on the whole data analysis. However, in the spinal and pelvic district, ^{18}F -FDG PET/CT and MRI were comparable, and both performed better than ^{99m}Tc -MIBI in visualizing focal lesions. On the other hand, ^{99m}Tc -MIBI and MRI showed a higher rate of diffuse pattern detection compared with ^{18}F -FDG PET/CT both in the whole data and in the spinal and pelvic analysis. Because of the objective difficulty—for both practical and ethical reasons—in obtaining biopsy samples from each suspected lesion, our findings were interpreted in relation to the clinical context and analyzed to compare simultaneously the 3 imaging modalities. Moreover, previous studies showed that a whole-body radiographic survey—traditionally used in the Durie and Salmon staging system to detect lytic lesions—can significantly underestimate bone and bone marrow involvement, especially in newly diagnosed patients (4). Therefore, an independent “gold standard” of reference cannot be easily provided in this disease. Nevertheless, the 3 imaging methods singly or in combination influenced the subsequent clinical management in 18% of patients.

The higher number of focal lesions detected by ^{18}F -FDG PET/CT compared with ^{99m}Tc -MIBI (196 and 63 lesions, respectively) may be due to the mechanism of ^{18}F -FDG uptake that reflects the increased glycolysis usually occurring in tumor cells and, thus, the rapid growth and invasive characteristics of focal lesions (4,16,26)—though the inflammation that can be associated with tumor proliferation may also contribute to increased ^{18}F -FDG uptake (27). Moreover, the use of a hybrid system composed by PET and CT images allowed the detection of small or slightly active lesions that were barely distinguishable from the surrounding normal tissue on the basis of PET images alone (28). The hybrid system also allows a more precise anatomic localization of hypermetabolic lesions and, therefore, a better discrimination between bone and soft-tissue lesions (8,10). In fact, ^{18}F -FDG PET/CT detected a total of 18 soft-tissue lesions, whereas ^{99m}Tc -MIBI visualized only 3 of them. The resolution of ^{99m}Tc -MIBI could be improved by performing SPECT. This technique of acquisition, though, would be time-consuming and costly, taking from ^{99m}Tc -MIBI imaging some of its positive characteristics—technical ease,

rapidity of execution (the study is performed 10 min after injection and lasts only 10 min), and low costs.

On the whole data analysis, ^{18}F -FDG PET/CT detected more focal lesions than MRI (196 and 51 lesions, respectively) because of the presence of a consistent number of lesions outside the spine and pelvis (121 lesions detected by ^{18}F -FDG PET/CT and 53 lesions detected by ^{99m}Tc -MIBI). In fact, focusing our analysis exclusively on the spinal and pelvic district, the number of focal lesions visualized by ^{18}F -FDG PET/CT and MRI became comparable (75 and 51 lesions, respectively). In this district, both ^{18}F -FDG PET/CT and MRI performed better than ^{99m}Tc -MIBI, which detected 10 lesions only; this finding could be due to the physiologic uptake of ^{99m}Tc -MIBI in the liver and its excretion in the bowel, which may obscure local focal lesions (18).

^{99m}Tc -MIBI performed better than ^{18}F -FDG PET/CT in the detection of a diffuse pattern of bone marrow uptake both in the whole data (33% of patients by ^{99m}Tc -MIBI and 9% by ^{18}F -FDG PET/CT) and in the spinal and pelvic analysis (54% of patients by ^{99m}Tc -MIBI and 18% by ^{18}F -FDG PET/CT). The meaning of ^{18}F -FDG diffuse bone marrow uptake in MM patients must be further investigated, as a mild and diffuse ^{18}F -FDG uptake in the spine could be also found in young or mildly anemic patients (28,29). On the other hand, previous studies showed that ^{99m}Tc -MIBI concentrates in malignant plasma cells and that diffuse tracer uptake correlates with the percentage of plasma cell infiltration and the amount of a monoclonal component (13,15). Moreover, it has been shown that ^{99m}Tc -MIBI bone marrow uptake is able to identify active myeloma and that the extension and intensity of tracer uptake correlates both with the clinical status and the stage of disease (13). In fact, a previous study showed that moderate-to-intense diffuse ^{99m}Tc -MIBI uptake or focal uptake with or without diffuse uptake, in the absence of inflammation or other pathologies, excludes the diagnosis of monoclonal gammopathy of unknown significance (MGUS) and correlates with poor prognosis (19). However, it should be noted that faint bone marrow uptake has been reported also in patients affected by pathologies other than MM (20). Nevertheless, when the intensity of diffuse ^{99m}Tc -MIBI uptake was analyzed according to the criteria used by Pace et al. (13), specificity improved significantly (20). False-negative cases by ^{99m}Tc -MIBI may be due, rather, to the overexpression of P-glycoprotein (Pgp) that can be associated with multidrug-resistant myeloma. ^{99m}Tc -MIBI, in fact, is a transport substrate of the energy-dependent efflux pump Pgp, and its washout increases over time from the bone marrow of MM patients overexpressing this protein (17,30). Therefore, to overcome the action of Pgp in our study, imaging was performed no later than 10 min after the injection of ^{99m}Tc -MIBI.

Similarly to ^{99m}Tc -MIBI, MRI also performed better than ^{18}F -FDG PET/CT in the detection of a diffuse pattern both in the whole data and in the spinal and pelvic analysis (39% of patients by MRI of spine and pelvis, 9% by whole-body ^{18}F -FDG PET/CT, and 18% by ^{18}F -FDG PET/CT in the spinal

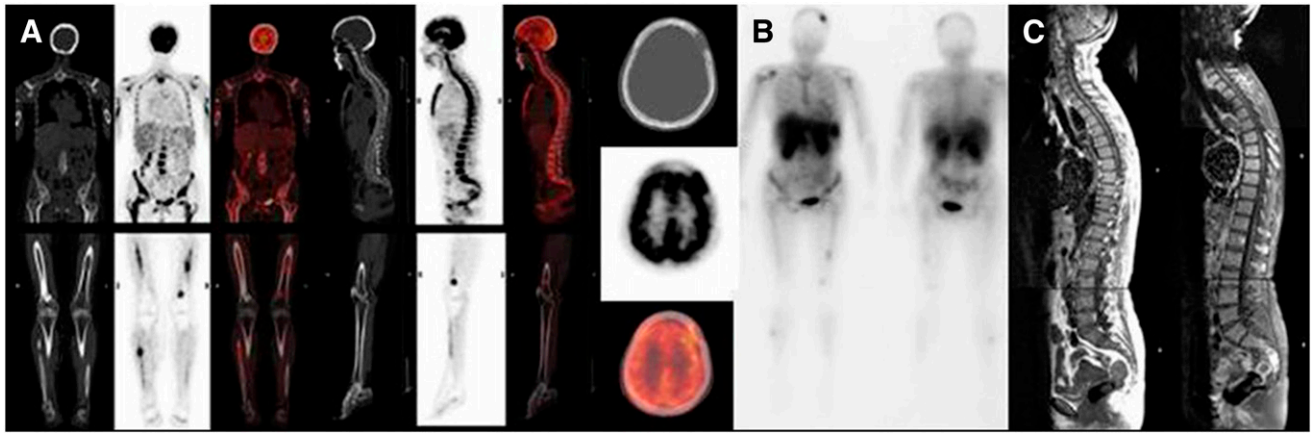


FIGURE 1. Coronal, sagittal, and transaxial CT, PET, and fused images of whole-body ^{18}F -FDG PET/CT (A), anterior and posterior whole-body $^{99\text{m}}\text{Tc}$ -MIBI (B), and sagittal T1- and T1-weighted fat-saturated with gadolinium MR images of spine (C). All 3 imaging modalities, performed on the same MM patient, showed a focal + diffuse pattern of distribution. In particular, focal lesions were shown in skull, humeri, pelvis, left femur, and right fibula by whole-body ^{18}F -FDG PET/CT; in skull, right humerus, pelvis, left femur, and right fibula by whole-body $^{99\text{m}}\text{Tc}$ -MIBI; and in coccygeal bone by MRI of spine and pelvis.

and pelvic regions, respectively). Previous studies, in fact, showed that a diffuse pattern of distribution detected by MRI in MM patients correlates with increased bone marrow cellularity, increased plasmacytosis (although $<10\%$ may be associated with false-negative cases), anemia, and poorer survival (31). Moreover, recent studies showed that MRI was more sensitive than ^{18}F -FDG PET/CT in the detection of an infiltrative pattern, allowing direct visualization of the bone content with a high spatial resolution (8,28). These features can be useful, especially in the spinal and pelvic regions that have a complex anatomy and are overlaid by bowel and ribs, respectively (32)—though, the field of view of MRI excludes regions such as skull, sternum, ribs, and long bones containing a high amount of red marrow and frequently infiltrated by malignant plasma cells (23,24), as shown in Figure 1. In fact, it has been shown that in substituting a whole-body radiographic survey with MRI of spine and pelvis, 10% of MM patients would be understaged (33). In this respect, Zamagni et al. (8) reported that MRI was superior to ^{18}F -FDG PET/CT in the assessment of bone marrow involvement of the spine and pelvis, whereas ^{18}F -FDG PET/CT allowed the detection of myelomatous lesions that were out of the field of view of MRI. In agreement with these findings, our study showed that MRI performed better than ^{18}F -FDG PET/CT in the evaluation of diffuse disease and performed equally well in the detection of focal disease in the spinal and pelvic regions. Also, our study showed a considerable number of focal lesions detected by ^{18}F -FDG PET/CT that were out of the field of view of MRI. This limitation could be overcome by using whole-body MRI. Currently, though, this imaging technique is not widely available yet, and its imaging times are still too long despite the advances in MRI, such as the development of rapid data acquisition and high-performance gradient systems (9). Moreover, the spatial resolution of whole-body MRI is worse than that of focused surface-coil MRI, resulting in poorer imaging quality (34).

CONCLUSION

In whole-body analysis, ^{18}F -FDG PET/CT and $^{99\text{m}}\text{Tc}$ -MIBI provided complementary information in the diagnostic evaluation of MM patients by detecting focal and diffuse disease, respectively. In the spinal and pelvic regions, MRI was comparable to ^{18}F -FDG PET/CT and $^{99\text{m}}\text{Tc}$ -MIBI in the detection of focal and diffuse patterns, respectively. Therefore, in the diagnostic work-up of multiple myeloma, MRI—because of its ability in detecting both focal and diffuse disease in the spine and pelvis—should be reserved for the evaluation of bone marrow involvement in these regions. Until whole-body MRI with reasonably short imaging times, good spatial resolution, and standardized sequences for MM will be widely available, the main drawback of MRI of spine and pelvis will be the limited field of view that could understage newly diagnosed MM patients, by missing lesions located outside these regions. Therefore, in the whole-body evaluation of MM patients at diagnosis, ^{18}F -FDG PET/CT can contribute to a more accurate assessment of disease—especially in a clinical context highly suggestive of focal involvement of the appendicular skeleton, such as the presence of bone pain or pathologic fractures in long bones or in the case of discrepancies between clinical status and hematologic parameters. On the other hand, despite the limited capacity in detecting focal lesions, $^{99\text{m}}\text{Tc}$ -MIBI still remains the most rapid and inexpensive technique for whole-body evaluation and may be an alternative option when a PET facility is not available.

ACKNOWLEDGMENTS

This work was partly supported by EU grant EMIL (European Molecular Imaging Laboratories Network) contract 503569, by the Ministry of Health, and by the Ministry of University and Research.

REFERENCES

- Malpas JS, Carroll JJ. Myeloma: clinical presentation and diagnosis. In: Malpas JS, Bergsagel DE, Kyle RA, eds. *Myeloma: Biology and Management*. New York, NY: Oxford University Press; 1995:169–190.
- Angtuaco EJ, Fassas AB, Walker R, Sethi R, Barlogie B. Multiple myeloma: clinical review and diagnostic imaging. *Radiology*. 2004;231:11–23.
- Durie BG, Salmon SE. A clinical staging system for multiple myeloma: correlation of measured myeloma cell mass with presenting clinical features, response to treatment and survival. *Cancer*. 1975;36:842–854.
- Durie BG, Waxman AD, D'Agnolo A, Williams CM. Whole-body ¹⁸F-FDG PET identifies high-risk myeloma. *J Nucl Med*. 2002;43:1457–1463.
- Smith A, Wisloff F, Samson D, Myeloma Forum UK; Nordic Myeloma Study Group. British Committee for Standards in Haematology: Guidelines on the diagnosis and management of multiple myeloma 2005. *Br J Haematol*. 2006;132:410–451.
- Durie BG. The role of anatomic and functional staging in myeloma: description of Durie/Salmon plus staging system. *Eur J Cancer*. 2006;42:1539–1543.
- D'Sa S, Abildgaard N, Tighe J, Shaw P, Hall-Craggs M. Guidelines for the use of imaging in the management of myeloma. *Br J Haematol*. 2007;137:49–63.
- Zamagni E, Nanni C, Patriarca F, et al. A prospective comparison of ¹⁸F-fluorodeoxyglucose positron emission tomography-computed tomography, magnetic resonance imaging and whole-body planar radiographs in the assessment of bone disease in newly diagnosed multiple myeloma. *Haematologica*. 2007;92:50–55.
- Mulligan ME, Badros AZ. PET/CT and MR imaging in myeloma. *Skeletal Radiol*. 2007;36:5–16.
- Beyer RJ 3rd, Mulligan ME, Smith SE, Line BR, Badros AZ. Comparison of imaging with FDG PET/CT with other imaging modalities in myeloma. *Skeletal Radiol*. 2006;35:632–640.
- Tirovola EB, Biassoni L, Britton KE, Kaleva N, Kouykin V, Malpas JS. The use of ^{99m}Tc-MIBI scanning in multiple myeloma. *Br J Cancer*. 1996;74:1815–1820.
- el-Shirbiny AM, Yeung H, Imbriaco M, Michaeli J, Macapinlac H, Larson SM. Technetium-99m-MIBI versus fluorine-18-FDG in diffuse multiple myeloma. *J Nucl Med*. 1997;38:1208–1210.
- Pace L, Catalano L, Pinto A, et al. M. Different patterns of technetium-99m sestamibi uptake in multiple myeloma. *Eur J Nucl Med*. 1998;25:714–720.
- Catalano L, Pace L, Califano C, et al. Detection of focal myeloma lesions by technetium-99m-sestamibi scintigraphy. *Haematologica*. 1999;84:119–124.
- Fonti R, Del Vecchio S, Zannetti A, et al. Bone marrow uptake of ^{99m}Tc-MIBI in patients with multiple myeloma. *Eur J Nucl Med*. 2001;28:214–220.
- Mileshkin L, Blum R, Seymour JF, Patrikeos A, Hicks RJ, Prince HM. A comparison of fluorine-18 fluoro-deoxyglucose PET and technetium-99m sestamibi in assessing patients with multiple myeloma. *Eur J Haematol*. 2004;72:32–37.
- Pace L, Catalano L, Del Vecchio S, et al. Washout of (^{99m}Tc) sestamibi in predicting response to chemotherapy in patients with multiple myeloma. *Q J Nucl Med Mol Imaging*. 2005;49:281–285.
- Hung GU, Tsai CC, Tsai SC, Lin WY. Comparison of Tc-99m sestamibi and F-18 FDG-PET in the assessment of multiple myeloma. *Anticancer Res*. 2005;25:4737–4741.
- Martin MG, Romero Colas MS, Dourdil Sahun MV, Olave P, Alba PR, Banzo JB. Baseline Tc99-MIBI scanning predicts survival in multiple myeloma and helps to differentiate this disease from monoclonal gammopathy of unknown significance. *Haematologica*. 2005;90:1141–1143.
- Nandurkar D, Kalff V, Turlakow A, Spencer A, Bailey MJ, Kelly MJ. Focal MIBI uptake is a better indicator of active myeloma than diffuse uptake. *Eur J Haematol*. 2006;76:141–146.
- Mele A, Offidani M, Visani G, et al. Technetium-99m sestamibi scintigraphy is sensitive and specific for the staging and the follow-up of patients with multiple myeloma: a multicentre study on 397 scans. *Br J Haematol*. 2007;136:729–735.
- Erten N, Saka B, Berberoglu K, et al. Technetium-99m 2-methoxy-isobutylisonitrile uptake scintigraphy in detection of the bone marrow infiltration in multiple myeloma: correlation with MRI and other prognostic factors. *Ann Hematol*. 2007;86:805–813.
- Schmidt GP, Schoenberg SO, Reiser MF, Baur-Melnyk A. Whole-body MR imaging of bone marrow. *Eur J Radiol*. 2005;55:33–40.
- Lucignani G. Bone and marrow imaging: do we know what we see and do we see what we want to know? *Eur J Nucl Med Mol Imaging*. 2007;34:1123–1126.
- Durie BG, Kyle RA, Belch A, et al. Myeloma management guidelines: a consensus report from the Scientific Advisors of the International Myeloma Foundation. *Hematol J*. 2003;4:379–398.
- Bredella MA, Steinbach L, Caputo G, Segall G, Hawkins R. Value of FDG PET in the assessment of patients with multiple myeloma. *AJR*. 2005;184:1199–1204.
- Jadvar H, Conti PS. Diagnostic utility of FDG PET in multiple myeloma. *Skeletal Radiol*. 2002;31:690–694.
- Nanni C, Zamagni E, Farsad M, et al. Role of ¹⁸F-FDG PET/CT in the assessment of bone involvement in newly diagnosed multiple myeloma: preliminary results. *Eur J Nucl Med Mol Imaging*. 2006;33:525–531.
- Schirmeister H, Buck AK, Bergmann L, Reske SN, Bommer M. Positron emission tomography (PET) for staging of solitary plasmacytoma. *Cancer Biother Radiopharm*. 2003;18:841–845.
- Fonti R, Del Vecchio S, Zannetti A, et al. Functional imaging of multidrug resistant phenotype by ^{99m}Tc-MIBI scan in patients with multiple myeloma. *Cancer Biother Radiopharm*. 2004;19:165–170.
- Mouloupoulos LA, Gika D, Anagnostopoulos A, et al. Prognostic significance of magnetic resonance imaging of bone marrow in previously untreated patients with multiple myeloma. *Ann Oncol*. 2005;16:1824–1828.
- Baur-Melnyk A, Buhmann S, Durr HR, Reiser M. Role of MRI for the diagnosis and prognosis of multiple myeloma. *Eur J Radiol*. 2005;55:56–63.
- Lecouvet FE, Malghem J, Michaux L, et al. Skeletal survey in advanced multiple myeloma: radiographic versus MR imaging survey. *Br J Haematol*. 1999;106:35–39.
- Johnston C, Brennan S, Ford S, Eustace S. Whole body MR imaging: applications in oncology. *Eur J Surg Oncol*. 2006;32:239–246.